General Disclaimer

One or more of the Following Statements may affect this Document

- This document has been reproduced from the best copy furnished by the organizational source. It is being released in the interest of making available as much information as possible.

- This document may contain data, which exceeds the sheet parameters. It was furnished in this condition by the organizational source and is the best copy available.

- This document may contain tone-on-tone or color graphs, charts and/or pictures, which have been reproduced in black and white.

- This document is paginated as submitted by the original source.

- Portions of this document are not fully legible due to the historical nature of some of the material. However, it is the best reproduction available from the original submission.

Produced by the NASA Center for Aerospace Information (CASI)

NASA CR- 144829

18

22 NOVEMBER 1976

LANDSAT D

POSITION DETERMINATION AND CORRECTION STUDY

(NASA-CR-144829) LANDSAT D POSITION DETERMINATION AND CORRECTION STUDY Final Report (General Electric Co.) 30 p HC A03/MF A01 CSCL 08B

N77-13496

Unclas

G3/43 58217

FINAL REPORT

Prepared for

THE NATIONAL AERONAUTICS AND SPACE ADMINISTRATION
GODDARD SPACE FLIGHT CENTER
GREENBELT, MARYLAND 20771

DEC 1976
RECEIVED
NASA STI FACILITY
INPUT BRANCH

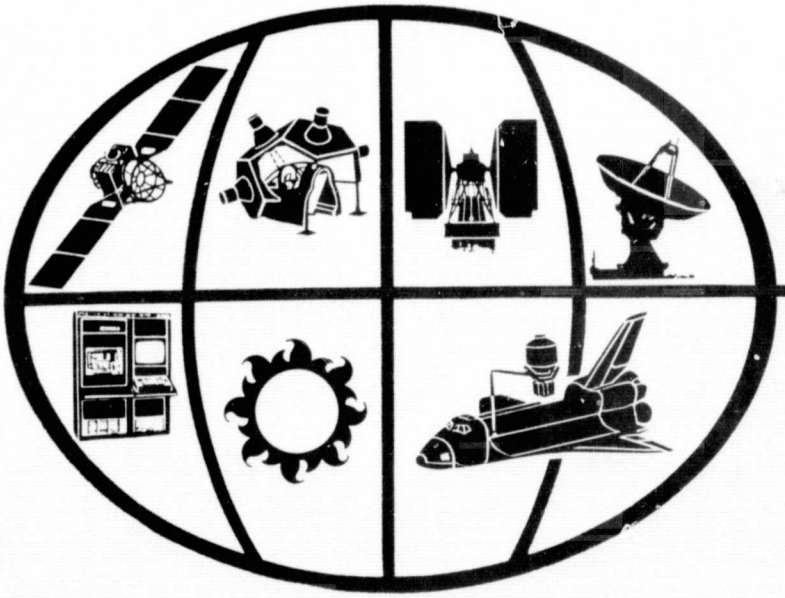

space division

CONTRACT NO. NAS 5-23412, Mod 12
GE DOCUMENT NO. 76SDS4277

GENERAL ELECTRIC

This final report is submitted by the General Electric Space Division in partial satisfaction of the contractual requirements of Contract NAS 5-23412, Modification 12.

The technical contributors to this report include:

A. Aaronson	J. Boytim	R. Fries	W. Phillips
T. Aepli	C. Cahill	K. Han	S. Schramm
L. Alexander	R. Cox	A. Kitto	R. Sergo
A. Alley	W. Dallam	G. Liebling	K. Speight
B. Bachofer	J. Echard	W. Lott	R. Spencer
R. Baker	R. Ferguson	D. Merz	K. Stow
R. Boram	P. Fischer	A. Park	

APPROVED BY: W Kent Stow

W. Kent Stow
Program Manager

Any questions or comments regarding this report should be addressed to:

W. Kent Stow
Program Manager
General Electric-Space Division
P.O. Box 8555
Philadelphia, Pa. 19101
(215) 962-2487

Dr. Thomas Lynch
Technical Officer, Code 930
NASA Goddard Space Flight Center
Greenbelt, Maryland, 20771
(301) 982-6445

TABLE OF CONTENTS

SECTION		PAGE
1	INTRODUCTION AND SUMMARY	1
	1.1 Background	1
	1.2 The Landsat D Ground System	5
	1.3 Position Determination and Correction Summary	7
2	ERROR ANALYSIS	8
	2.1 Basic Assumptions	8
	2.2 Error Sources	8
	2.2.1 Attitude Control	8
	2.2.2 Ephemeris	10
	2.2.3 Alignment	11
	2.2.4 Other Error Sources	12
3	CORRECTION PROCESSING	13
	3.1 Implementation Scheme	13
	3.2 Correction Functions	16
	3.3 Control Point Transformations	17
	3.4 Map Projections	19
4	CONCLUSIONS	24
	REFERENCES	25

LIST OF ILLUSTRATIONS

FIGURE NO.		PAGE
1-1	Landsat D System	2
1-2	Ground System Concept	5
2-1	Attitude Control Induced Errors	9
2-2	Geometric Errors Introduced by Ephemeris Uncertainties	10
2-3	Errors Introduced by Alignment Uncertainties	11
2-4	Errors Introduced by Other System Uncertainties	12
3-1	The Affine Transformation	18
3-2	Universal Transverse Mercator Projection	19
3-3	Space Oblique Mercator Projection	20
3-4	Lambert Conformal Conic Projection	21
3-5	Scene Orientation at the Equator	22
3-6	Rotational Buffer Cost	23

TABLE NO.		
2-1	Error Source Summary	9
3-1	Residual Geometric Errors After GCP Correlation	15

SECTION 1

INTRODUCTION AND SUMMARY

1.1 BACKGROUND

The pressing need to better survey and manage the earth's resources and environment has prompted man to explore the possibilities of remote sensing from space. Early efforts began with space photographs from the Gemini and Apollo programs and continued with multispectral data from Landsat 1 and 2 spacecraft. Landsat D is currently planned as the next major step for the Earth Resources Program.

Landsat 1, launched in 1972, marked the start of NASA's Earth Resources satellite program. This successful spacecraft was followed two and a half years later with Landsat 2, an identical spacecraft. The overwhelming success of these two Landsats, demonstrated through hundreds of experimental programs, has motivated NASA to continue to improve the Earth Resources satellite program. The third satellite, Landsat C, has been procured and is scheduled for launch in late 1977. This third satellite will carry a modified Multispectral Scanner and will utilize an improved digital ground system. NASA is now planning for the next step, Landsat D, which will provide several major advances. Landsat D will incorporate the Thematic Mapper (TM) as a new sensor, it will utilize the Multi-mission Modular Spacecraft (MMS), it will make use of the Tracking and Data Relay Satellite System (TDRSS) and it will employ a new more advanced ground system. Each of these represent significant improvements in the state-of-the-art. This study is one of several which address various aspects of the planned Landsat D system.

As the Earth Resources Program has matured through the Landsat spacecraft it has begun the transition from an experimental research activity to a sound demonstration of proven utility. This important transition will be completed with the Landsat D system which incorporates several key improvements over the current system. These improvements, based on experience with the existing Landsats, will provide new capabilities in the spacecraft, the sensor, the ground system, and the overall system design. These system

capabilities - which emphasize improved vegetation analysis, prompt availability of data, frequent coverage, and precise data registration and overlay for better change detection will permit the Landsat D to capture already proven economic benefits in such diverse applications as:

- Monitoring world-wide food productivity
- Mapping agricultural land use
- Monitoring rangelands
- Surveying forest resources
- Managing critical watersheds
- Detecting land use changes
- Oil/mineral exploration

An artist's concept of the Landsat D system is shown in Figure 1-1. The spacecraft will be based on NASA's new Multi-mission Modular Spacecraft (MMS) and will operate two remote sensing instruments: a Thematic Mapper (TM), with 30 meter ground resolution, and a Multispectral Scanner (MSS), with 80 meter resolution. The system provides two data communication paths to the Earth; one is a direct readout link for ground stations (both

Figure 1-1. Landsat D System

domestic and foreign) within range of the spacecraft, and the other is a relay link via the Tracking and Data Relay Satellite System (TDRSS) for nearly full global coverage. The spacecraft will be in a sun-synchronous orbit with a descending node time of 9:30 AM (similar to current Landsats). The orbital altitude and inclination will provide near global coverage of the land and near coastal regions with a repeat cycle every 16 to 18 days.

The use of the new MMS spacecraft as the basic bus will provide both improved sensor pointing accuracy (±0.01 degree) and stability (10^{-6} degrees/second). These improvements will manifest themselves in more accurate and more straightforward geometric corrections of the image data; both relative (image to image) and absolute (with respect to the Earth's surface). The MMS incorporates modular subsystems in the key areas of power, attitude control, and command and data handling. This modularity together with the compatibility for both conventional and Space Shuttle launches will enable in-orbit repair and refurbishment of the spacecraft.

The Thematic Mapper, TM, is an evolutionary improvement of the MSS and provides several significant capabilities. The spatial resolution on the ground has been reduced to 30 meters (compared to 80 for the MSS) which will allow radiances to be measured for areas (pixels) less than one sixth the size as for the MSS. The TM will incorporate six spectral bands (and have the capability for a seventh) which have been located primarily on the basis of their ability to discriminate vegetation (a fundamental application of remote sensing). In addition the radiometric sensitivity of the TM has been improved by reducing the signal-to-noise characteristic and increasing the levels of digital quantization. These sensor changes combine to cause the TM to have a data rate of 120 Mbps, (an order of magnitude increase over the 15 Mbps of the MSS).

For remotely sensed multispectral data to be truly practical for many potential operational users (agricultural analysts, hydrologists, etc.) it must be received by them in usable form within 48 to 96 hours after imaging. Promptness in receiving data products is one of the most critical aspects of the Landsat System.

The Landsat D System will be thoroughly integrated with the needs of operational users. It will include improved preprocessing of all data, central data processing, archiving and retrieval,

low-cost receiving and data centers for large volume users (such as the U. S. Department of Agriculture) and provide maximum efficiency and economy in utilization by state, regional, and foreign users. Featuring the rapid electronic transmission of all data, the Landsat D system will reduce the time between satellite imaging and user reception of data to the required 48 to 96 hours.

As illustrated in the artist's concept the system provides two data links to the ground. The first link, for both MSS and Thematic Mapper data, is directly from the satellite to domestic and foreign ground stations as the satellite passes through their reception areas. The second link is via the Tracking and Data Relay Satellite System (TDRSS). As shown, the data is transmitted to a TDRSS satellite, in stationary orbit, and relayed to the TDRSS receiving station. The TDRSS receiving station transmits the data via a domestic communications satellite to a central data processing facility that, in turn, relays the data to any local data distribution center equipped to receive it. This link, via TDRSS and the communications satellite, will thus have global acquisition and relay capabilities, providing rapid access to Thematic Mapper data for users throughout the world. Both data links have a planned maximum data capability of 135 Mb/second at a 10^{-5} bit error rate.

The Landsat D system described is currently in the planning stages by NASA. As part of the planning for this future system, NASA has undertaken a series of studies, with General Electric and others, to investigate various system options. This particular study is one of seven conducted by General Electric to explore different aspects of the total ground system that will be required by Landsat D in order to meet the overall mission objectives.

The seven ground system studies are:

1. Local User Terminal Study - an investigation into the requirements and options available for direct readout (primarily foreign ground stations) of Landsat D data.

2. User Data Processing Study - an effort to estimate the scope, size, and cost of the major user data processing system requirements.

3. Data Processing Facility Study - a requirement and sizing study to provide preliminary estimates of the scope and cost of NASA's central Landsat D data processing center.

4. GSFC Research & Development Study - a survey and analysis of the functions and facility required of NASA to continue the basic research on spaceborne remote sensing and its applications.

5. Operation Control Study - an analysis of the modifications necessary to upgrade or modify the NASA Operations Control Center (OCC) for Landsat D.

6. Data Transmission and Dissemination Study - an investigation into the options and limitations of various data communication alternatives including centralization versus decentralization.

7. Position Determination and Correction Study - an analysis of the impact and alternatives afforded by the MMS spacecraft of Landsat D on image geometric correction.

1.2 THE LANDSAT D GROUND SYSTEM

A top-level functional diagram of the Landsat D ground system is presented in Figure 1-2. The five major subsystems included are the Data Input Subsystem (DIS), the Central Data Processing Facility (CDPF), the Product Generation and Dissemination Facility (PGDF), the Data Management Subsystem (DMS), and the Agriculture Utilization Subsystem (AUS). Each of these subsystems is briefly described below.

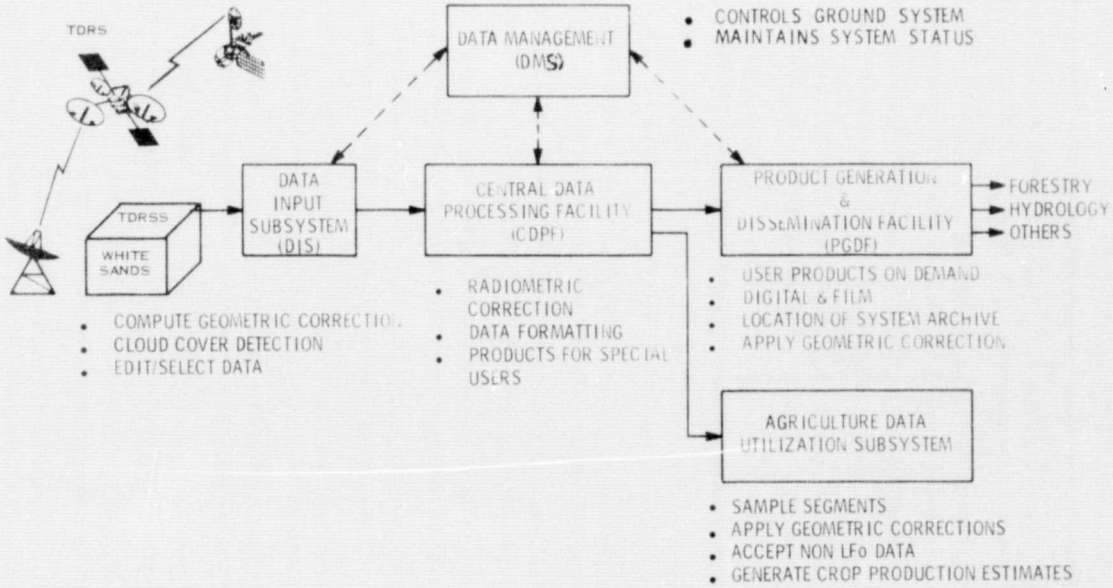

Figure 1-2. Ground System Concept

The Data Input Subsystem (DIS) receives 120-135 Mbps data from the TDRSS via dedicated cable interconnection. The prime functions of the DIS are to record the raw input data, to perform cloud cover detection and scene editing, and to compute geometric correction matrices on a per swath basis.

The Central Data Processing Facility (CDPF) receives edited data from the DIS and performs standard operations to all data. These operations include radiometric correction and data reformatting to a band-interleaved-by-line (BIL) format.

The Product Generation and Dissemination Facility (PGDF) is the main interface between the Landsat D ground system and general users. This facility provides Landsat D data, in either digital tape or film format, to users on demand. The data, which may be geometrically corrected to various map projection systems or enhanced as requested by the user, is available in a variety of sizes, formats, and media. The PGDF also houses and manages the system archive.

The Data Management Subsystem (DMS) provides the central point of control and data base management for the Landsat D ground system. Its prime functions include management of user demand, the system archive, system communications, and system redundancy. The DMS also maintains system status, production statistics, operations logs and administrative services.

The Agriculture Utilization Subsystem (AUS) receives data directly from the CDPF and performs those operations necessary to produce world crop production forecasts on a periodic basis. The operations to be performed include geometric correction, sample segment extraction, multispectral analysis, and areal and statistical analyses. It is included here as part of the ground system because it represents the first major user of Landsat D data.

Several other major subsystems included as part of the Landsat D ground system were considered. These include the Operations Control Center (OCC), the GSFC Research and Development Facility, and the Hydrologic Land-Use Utilization Subsystem. The OCC performs the functions required to plan, schedule, operate and evaluate spacecraft and payload

operations. The R&D Facility enables NASA to perform research related to the Landsat program and its applications. The Hydrologic/Land Use Utilization Subsystem is similar in concept to the AUS and will generate land use maps over watershed areas within the US.

1.3 POSITION DETERMINATION AND CORRECTION SUMMARY

The Landsat D system will require a significantly more accurate method of determining the geometric correction functions for image data than is currently available. In addition, more timely transmission of ephemeris data to the geometric correction process will be dictated by the operational nature of many of the anticipated user programs.

Use of the Multi-mission Modular Spacecraft (MMS) as the basic space vehicle for the Landsat D program will result in a considerable improvement in attitude control capability over current (Landsat 1 and 2) vehicles. In spite of this improvement, the vehicle attitude is still the overriding error source in the ability to determine the precise ground location of the sensor's instantaneous field of view. This means that predicted ephemeris, available 24 hours ahead of data acquisition may be used for the position of the spacecraft in all geometric correction calculations.

The geometric accuracy of the Landsat-D imagery after simple corrections which model known error sources will be approximately 275 meters (RMS). Although this accuracy is significantly better than the present Landsat capability of 1-2 kilometers, the use of control points to correct the imagery, on a swath basis, will be required to improve the position and registration accuracies to approximately one-half pixel.

In addition to improved accuracy, swath correction (possible because of very low MMS attitude rates) results in about a one-hundred to one reduction in the number of control points required to be surveyed, stored in the data base and correlated.

The report provides an assessment of accuracy of the knowledge of Landsat D spacecraft ephemeris data, an evaluation of the impact of expected attitude and alignment accuracies and analysis of the various options for the combining of precision ephemeris and attitude data with scene image data. Finally, this report will characterize the potential geometric correction system in order to determine overall system costs and impact on other system elements.

SECTION 2

ERROR ANALYSIS

2.1 BASIC ASSUMPTIONS

Position accuracy is defined as the ability to relate a point in the image to its true position on the earth's surface as represented by some map projection. Registration accuracy is defined as the ability to overlay two images of the same ground point taken at different points in time. Throughout the following analysis, accuracies will be defined in terms of one sigma (or RMS) which refers to a 68.3 percent probability of occurrence. Since the positional effects of some error sources are proportional to radial distance from the image center, RMS errors for such cases are represented by using the radial distance which delimits 68.3 percent of the image area. Where an error source causes both an X and Y positional shift, the vector sum is computed.

The Multi-mission Modular Spacecraft (MMS) will maintain its attitude in orbit to within $\pm 0.01^{\circ}$ (each axis) with a rate stability of $\pm 10^{-6}$ deg/sec. The payload will consist of two sensors; a five-band Multispectral Scanner (MSS) and a six-band Thematic Mapper (TM). Each sensor has a 185 km swath width. The instantaneous field of view on the ground for MSS is 79 meters and for TM is 30 meters.

2.2 ERROR SOURCES

The effect upon position accuracy of each major category of error source is shown in Table 2-1. This represents the system position accuracy after correction for earth rotation, initial alignment biases and sensor scan modeling. Compared to a 1-2 km error reported for Landsat 1 and 2 data, the Landsat-D system will perform three to seven times better even before control point analysis.

2.2.1 ATTITUDE CONTROL

The MMS is a very accurate and stable platform (see Reference 1). The RMS pointing specification (both knowledge and control) is ±0.01 degrees for each axis, which is fifty times better than Landsats 1 and 2. The RMS specification is 10^{-6} degrees/second for each axis, which

Table 2-1. Error Source Summary

Error Sources		Effect Upon Position Accuracy (After X & Y Translation & Rotation)
Attitude Control		175.2 Meters
Ephemeris		39.2
Alignment		206.4
Other	MSS	33.4
	TM	24.0

RSS Totals	MSS	275.6 (3.5 pixels)
	TM	274.6 (9.2 pixels)

is 15,000 times better than Landsats 1 and 2. This performance will be accomplished by star tracker updates every 5-10 minutes to the inertial reference unit.

Figure 2-1 shows the effect upon the image of each Attitude Control Subsystem, ACS, error source. The RSS total of all these error sources is 175.2 meters of position inaccuracy.

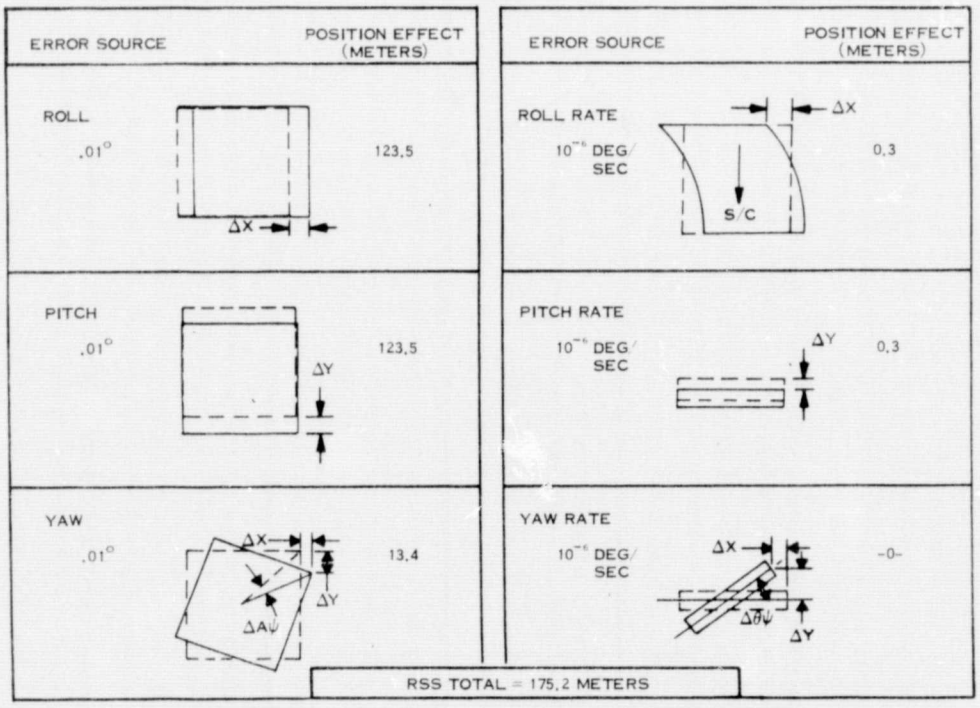

Figure 2-1. Attitude Control Induced Errors

2.2.2 EPHEMERIS

An analysis was performed by the Operational Orbit Support Branch at GSFC to determine the typical growth in radial, along track, and cross track prediction errors for Landsats 1 and 2 (reference 2). The results were obtained by predicting an orbit obtained from a two day definitive arc into the best four consecutive two day definitive arcs and extracting the maximum compare differences over days 1 through 8. The growth in prediction error is a function of the inability to model the effects of both atmospheric variations and the variable number of attitude gatings.

The RMS errors in predicted ephemeris after one day are shown in Figure 2-2 along with their effect upon position of the image. Also shown are the RMS errors in best fit ephemeris taken from an analysis done for Landsat C (reference 3). Since the total system position accuracy will improve by only two meters if best fit ephemeris is used instead of predicted, the baseline Landsat D system will use predicted ephemeris. This approach permits real time correction of the data, while use of best fit ephemeris causes delays of at least two days.

	PREDICTED			BEST FIT	
	ERROR SOURCE (METERS)	ACCURACY EFFECT (METERS)		ERROR SOURCE (METERS)	ACCURACY EFFECT (METERS)
INTRACK	34.3	34.3	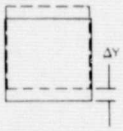	19.0	19.0
CROSSTRACK	19.0	19.0	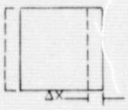	4.0	4.0
RADIAL	16.1	0.6		1.3	0.1
	RSS TOTAL = 39.2 METERS			RSS TOTAL = 19.4 METERS	

Figure 2-2. Geometric Errors Induced by Ephemeris Uncertainties

2.2.3 ALIGNMENT

The attitude control module will be aligned to the MMS structure to within ±200 arc seconds (RMS) in each axis (see reference 1). It is reasonable to assume that the payload module will be similarly aligned to the MMS so that the initial alignment bias between the sensor optical axis and vehicle pointing vector will be $\pm 200\sqrt{2}$ $\widehat{\text{sec}}$. This bias will be measured before launch and can be removed from the image data. The alignments are expected to vary over the orbital period by as much as $\pm 30\sqrt{2}$ $\widehat{\text{sec}}$ in each axis. This error source cannot be removed until control point analysis has modelled its positional effect as a function of time. Figure 2-3 shows the alignment error sources by magnitude and their effect upon position accuracy.

	INITIAL BIAS			STABILITY	
	ERROR SOURCE	POSITION EFFECT (METERS)		ERROR SOURCE	POSITION EFFECT (METERS)
ROLL	$200\sqrt{2}$ $\widehat{\text{SEC}}$	980.9	ΔX	$30\sqrt{2}$ $\widehat{\text{SEC}}$	145.5
PITCH	$200\sqrt{2}$ $\widehat{\text{SEC}}$	980.9	ΔY	$30\sqrt{2}$ $\widehat{\text{SEC}}$	145.5
YAW	$200\sqrt{2}$ $\widehat{\text{SEC}}$	106.0	ΔX, ΔY, ΔAV	$30\sqrt{2}$ $\widehat{\text{SEC}}$	15.7
	RSS TOTAL = 1391.2 METERS			RSS TOTAL = 206.4 METERS	

Figure 2-3. Errors Introduced by Alignment Uncertainties

2.2.4 OTHER ERROR SOURCES

Figure 2-4 lists the remaining error sources which contribute small but non-negligible amounts of position accuracy to the imagery. Spacecraft velocity will be known very accurately (reference 4), and its positional effect is not large. The knowledge of when the image was taken has been estimated very conservatively at ±1 msec. The vehicle altitude could change by as much as 200 meters between ephemeris updates causing a scale change in the cross-track direction as shown in the figure. The sensor scan is nonlinear and can be modelled so that residual errors are small. Internal source errors include such items as line start jitter, detector misalignments and scan-to-scan repeatability (see references 5 and 6).

ERROR SOURCE		EFFECT UPON POSITION ACCURACY (METERS)	
		MSS	TM
SPACECRAFT VELOCITY: INTRACK .133 M/SEC CROSSTRACK .133 RADIAL 2.0	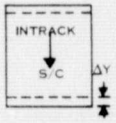	3.8 3.8 ---	3.7 3.7 ---
TIMING: 1 mSEC	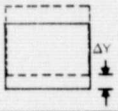	7.5	7.5
ALTITUDE CHANGE: 200 METER	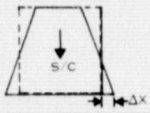	21.7	21.7
SCAN NONLINEARITIES:	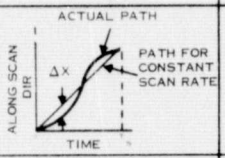	20.0	2.8
INTERNAL SENSOR		12.6	3.8
	RSS TOTALS	33.4	24.0

Figure 2-4. Errors Introduced by Other System Uncertainties

SECTION 3

CORRECTION PROCESSING

3.1 IMPLEMENTATION SCHEME

The errors present in the Landsat D attitude, ephemeris and alignment data make it necessary to establish ground truth before more precise correction is possible. By determining the image coordinates of well defined geographic features to be used as Ground Control Points (GCP's) in the scene, the correspondence between image coordinates and the actual control point location on the earth's surface can be used to compute correction functions.

Search areas will be established throughout a swath where it is most likely that high contrast, cloud free, control points will be present in one Thematic Mapper band. The map coordinates of these search areas are adjusted for earth rotation, earth curvature, initial alignment biases, and sensor scan modeling. This is essentially an X and Y translation plus a rotation correction which reduces the location error to 275 meters. If a search area of 10 by 10 pixels is used, then the probability that the GCP is present within the search area will be 68.3%.

The image coordinates of a ground control point are the sample and line numbers in the digital data. There are many techniques which could be used to determine the image coordinates. Most automated techniques require that subimages of the selected geographic features (window areas) have been identified in other Landsat scenes and entered into a ground control point library. One of the candidate techniques (e.g. Sequential Similarity Detection Algorithm (SSDA), Edge Detection or Fast Fourier Transform) will be applied to the image data in order to locate GCP's. SSDA employs a random sampling sequence for comparing window area pixels with search area pixels; test results using this technique on Landsat data are available in reference 7. Fast Fourier Transform techniques compute the mathematical cross-correlation of the two images and register them where the correlation surface peaks (see reference 8). Edge detection and correlation are currently used to correct Landsat images for the LACIE project.

On the basis of the positions of GCP's in the image, and their known geographic location, a least squares fit (or affine transformation) is computed, which results in a mapping function (global mapping polynomial) to be used to compute the image coordinates for every pixel position in the corrected image.

Since computation becomes excessive if the mapping polynomial is computed for the more than 37 million pixels in one Thematic Mapper image, relatively few interpolation grid points (anchor points) will be mapped with the full mapping function. The other output image points will be located by bilinear interpolation from these anchor points. The interpolation grid is selected so that the errors in interpolation are no more than 0.25 pixel.

After a point in the output plane has been mapped into the input image plane, a radiometric intensity must be assigned to it. In general, the distorted image plane will not have a radiometric intensity corresponding to the point mapped from the output plane. This requires that the input plane be resampled at the output point locations to obtain the correct intensities. Studies have shown that cubic convolution resampling produces less error than either nearest neighbor or bilinear interpolation (see reference 9).

Corrections may be applied to the image data as requested by the users, or data tapes may be supplied with the correction coefficients as a header. The expected accuracies in the data after control point processing are shown in Table 3-1, as a function of the number of control points correlated per swath. All errors are one-sigma (RMS) values in terms of meters on the ground. The GCP correlation error can vary from 0.3-0.8 pixels depending upon how much the image is obscured by clouds, haze or noise (see reference 8). At a USGS map scale of 1:24,000, National Map Accuracy Standards require that landmarks be displayed within 0.5 mm of their true position. The error in reading the true GCP coordinates from a map is therefore 12 meters. Both of these errors will reduce by a factor related to the square root of the number of control points.

Table 3-1. Residual Geometric Errors After GCP Correlation

Error Source	Residual Errors (Meters)			
	1 GCP	2 GCP's	4 GCP's	7 GCP's
Position Accuracy				
GCP Correlation Error	12.73-33.94	9.0 - 24.0	6.37 - 16.97	4.81-12.83
Map Location of Control Point 0.5 mm at 1:24000	12	8.49	6	4.54
Residual Yaw Error	13.4	13.4	12.19	9.92
Non-Linear Scan	5	5	5	5
Resampling Error (cubic convolution)	1	1	1	1
Grid Interpolation	4.3	4.3	4.3	4.3
Internal Sensor	4.6	4.6	4.6	4.6
	---	---	---	---
RSS	23-39	20-30	17-23	14-19
Registration Accuracy				
Remove GCP Map Location	12	8.49	6	4.54
	---	---	---	---
RSS	20-37	18-29	16-22	13-18

Simulations have been performed to determine yaw by using GCP's (see Reference 10), and the results are reflected in Table 3-1 above. In that same reference the Thematic Mapper scan profile was assumed to be modelled to an accuracy of 0.17 pixel (i.e. residual scan non-linearity of 5 meters.) GE correction systems use cubic convolution (sinX)/X resampling with a resolution of typically 1/16 pixel. The one-sigma resampling error is therefore $1/16\sqrt{3}$ pixels or one meter. The correction function for a scene is not computed for every pixel but for an array of points uniformly spaced over the scene. The correction value for

any given pixel is obtained by a bilinear interpolation of the surrounding array points. Experience at GE indicates that ±0.25 pixel is a realistic error having a uniform distribution ($7.5/\sqrt{3}$ meters). In reference 6 the internal TM sensor errors such as start of scan stability, across scan non-linearity and detector misalignments combine to 4.6 meters. When registering two images, the map coordinates of the control points are not relevant; thus the error due to map location is removed from the error budget shown in Table 3-1 above.

3.2 CORRECTION FUNCTIONS

Certain error sources can be removed from the data since they are known or predictable without recourse to control point analysis. Removal of these errors results in the 275 meter position accuracy described previously. The principal corrections are detailed in the following paragraphs.

Images become skewed as a result of the rotation of the earth during the finite frame time. The linear velocity of the earth at format center is

$$V = \frac{2 \text{ radians/day}}{86400 \text{ seconds/day}} \times R \times \cos L$$

where R = earth radius
L = latitude of format center

The inclination of the orbit to the local meridian at format center is

$$I = \sin^{-1} \left(\frac{\sin E}{\cos L}\right)$$

where E = orbit inclination at equator

The distortion components are therefore

$$\Delta X = V (\cos I) \ \Delta t$$
$$\Delta Y = V (\sin I) \ \Delta t$$

where Δt = time from format center

Thus, earth rotation correction is predictable and involves simple X and Y translations of the data.

The spacecraft axes are defined as follows: roll is coincident with the velocity vector, pitch is normal to the velocity vector parallel to the ground and yaw is the vertical axis of the spacecraft normal to the ground. Alignment biases in the roll axes result in the following image location errors:

$$\Delta X_r = H \ (\tan (B+\phi) - \tan B)$$
$$\Delta Y_r = 0$$

where H = S/C altitude
B = angle between S/C nadir and instantaneous field of view
ϕ = roll alignment bias

The errors resulting from pitch alignment biases are as follows:

$$\Delta X_p = 0$$
$$\Delta Y_p = H \tan \alpha$$

where α = pitch alignment bias

Position errors due to yaw alignment biases are:

$$\Delta X_y = X(1-\cos\gamma)$$
$$\Delta Y_y = X \sin \gamma$$

where X = distance from nadir to the ground point in the image
γ = yaw alignment bias

The sensor scan mechanism will deviate from the ideal linear case. Deviations from a linear scan profile can be determined empirically and incorporated into a scan model. The scan model can be applied to image data in order to reduce residual errors to a sub-pixel level.

3.3 CONTROL POINT TRANSFORMATIONS

As mentioned in paragraph 3.1 a mapping function is derived fromthe positions of control points in the output and image plane. Two likely candidates for use as mapping functions are the affine transformation and the least squares transformation.

The affine transformation is a mapping which accounts for distortions due to translation, scale change, rotation, aspect ratio and skew. To map a point from output plane to input image plane requires three GCP's which form a triangle containing that point. The detailed algorithm is shown in Figure 3-1 (from Reference 11.)

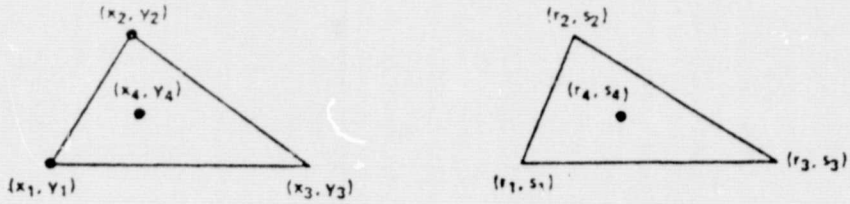

GIVEN ALL OF ABOVE EXCEPT (r_4, s_4). FIND (r_4, s_4)

1. FORM

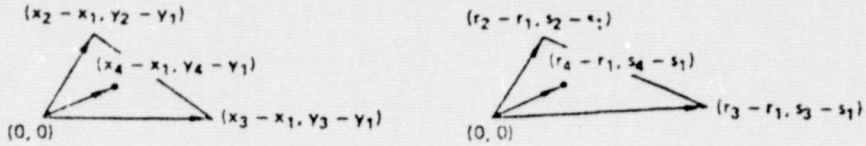

2. FIND MATRIX A SUCH THAT

$$\begin{bmatrix} a_{11} & a_{12} \\ a_{21} & a_{22} \end{bmatrix} \begin{bmatrix} x_2 - x_1 & x_3 - x_1 \\ y_2 - y_1 & y_3 - y_1 \end{bmatrix} = \begin{bmatrix} r_2 - r_1 & r_3 - r_1 \\ s_2 - s_1 & s_3 - s_1 \end{bmatrix}$$

SOLUTION

$$\begin{bmatrix} a_{11} & a_{12} \\ a_{21} & a_{22} \end{bmatrix} = \begin{bmatrix} r_2 - r_1 & r_3 - r_1 \\ s_2 - s_1 & s_3 - s_1 \end{bmatrix} \begin{bmatrix} \dfrac{y_3 - y_1}{d} & \dfrac{-(x_3 - x_1)}{d} \\ \dfrac{-(y_2 - y_1)}{d} & \dfrac{x_2 - x_1}{d} \end{bmatrix}$$

WHERE

$$d = (x_2 - x_1)(y_3 - y_1) - (y_2 - y_1)(x_3 - x_1)$$

NOTE: $d \neq 0$ IF FIGURE IS NOT A TRIANGLE

$$A = \begin{bmatrix} a_{11} & a_{12} \\ a_{21} & a_{22} \end{bmatrix} = \frac{1}{d} \begin{bmatrix} (r_2 - r_1)(y_3 - y_1) - (r_3 - r_1)(y_2 - y_1) & (r_3 - r_1)(x_2 - x_1) - (r_2 - r_1)(x_3 - x_1) \\ (s_2 - s_1)(y_3 - y_1) - (s_3 - s_1)(y_2 - y_1) & (s_3 - s_1)(x_2 - x_1) - (s_2 - s_1)(x_3 - x_1) \end{bmatrix}$$

3. FINALLY,

$$A \begin{bmatrix} x_4 - x_1 \\ y_4 - y_1 \end{bmatrix} = \begin{bmatrix} r_4 - r_1 \\ s_4 - s_1 \end{bmatrix}$$

SO

$$\begin{bmatrix} r_4 \\ s_4 \end{bmatrix} = \begin{bmatrix} r_1 \\ s_1 \end{bmatrix} + A \begin{bmatrix} x_4 - x_1 \\ y_4 - y_1 \end{bmatrix}$$

$$\begin{bmatrix} r_4 \\ s_4 \end{bmatrix} = \begin{bmatrix} r_1 \\ s_1 \end{bmatrix} + \begin{bmatrix} \{(x_4 - x_1)[(r_2 - r_1)(y_3 - y_1) - (r_3 - r_1)(y_2 - y_1)] + (y_4 - y_1)[(r_3 - r_1)(x_2 - x_1) - (r_2 - r_1)(x_3 - x_1)]\} / d \\ \{(x_4 - x_1)[(s_2 - s_1)(y_3 - y_1) - (s_3 - s_1)(y_2 - y_1)] + (y_4 - y_1)[(s_3 - s_1)(x_2 - x_1) - (s_2 - s_1)(x_3 - x_1)]\} / d \end{bmatrix}$$

Figure 3-1. Affine Transformation

ORIGINAL PAGE IS
OF POOR QUALITY

The other method of mapping involves the use of least squares polynomials. These polynomials have the form:

$$Z = C_o + C_1X + C_2Y + C_3X^2 + C_4XY + C_5Y^2 + C_6X^3 + C_7X^2Y + C_8XY^2 + C_9Y^3 + \ldots$$

The coefficients for these coefficients are computed from the GCP data with the minimum number of GCP's increasing with the degree of the polynomials. Also the placement of GCP's should be such that the corners and edges of the image area are covered to prevent large edge errors in the polynomial functions.

3.4 MAP PROJECTIONS

The user may be offered his choice of map projection, i.e. Universal Transverse Mercator (UTM), Space Oblique Mercator (SOM), and Lambert Conformal Conic (LCC).

In a transverse Mercator projection the Earth is projected onto a cylinder whose axis falls within the equatorial plane. The line of tangency between the Earth and the cylinder is along a longitude meridian. The Universal Transverse Mercator takes the cylinder's axis and rotates it in six degree steps as shown in Figure 3-2 (Reference 11). Thus the cylinder fits

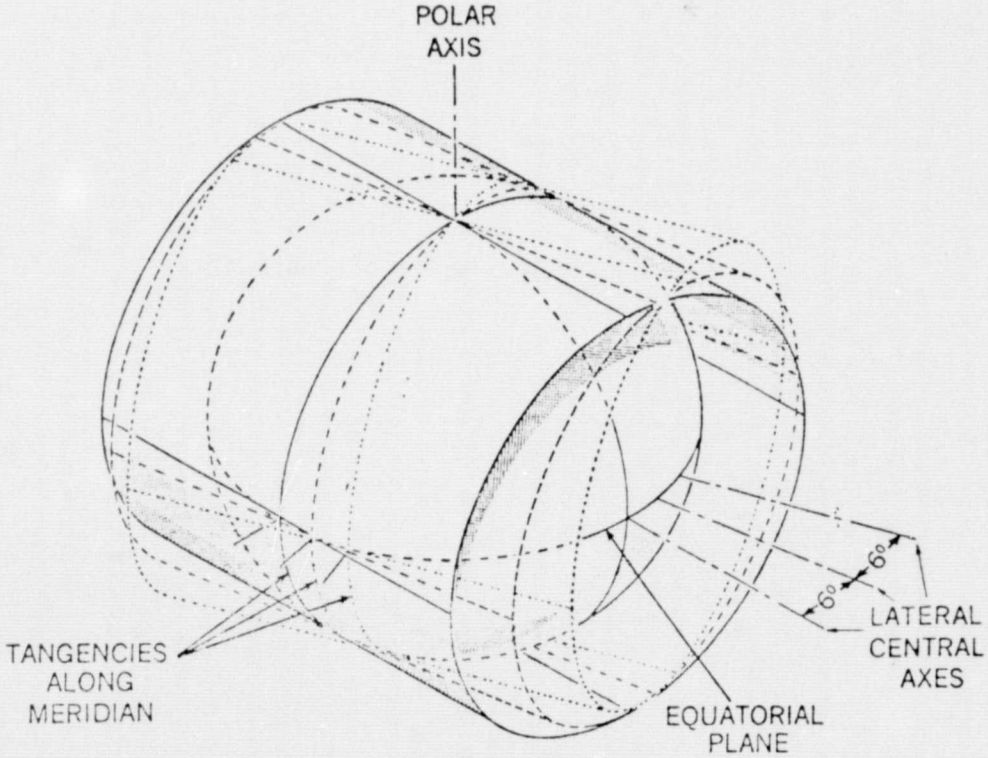

Figure 3-2. Universal Transverse Mercator Projection

the Earth's surface closely over ±3 degrees from the longitude of tangency for each UTM zone. Surface coordinates are measured in meters from the central target meridian and meters from the equator. The Northing and Easting coordinates together with the zone number define a point on the Earth's surface in UTM. Although it is not defined above 80° latitude, the UTM projection has the advantage of being a Cartesian coordinate system with identical units of measure along each axis. There is a disadvantage in terms of distortions due to projecting areas from one zone into the adjacent zone. This occurs at higher latitudes (above 60°) where the spacecraft heading angle increases at a rapid rate and the zone widths decrease causing a rapid traversing of zones. (For more detail see Reference 13).

The Space Oblique Mercator (SOM) projection involves a cylinder whose circumference is tangent to the satellite ground track as shown in Figure 3-3. It is defined in Reference 12.

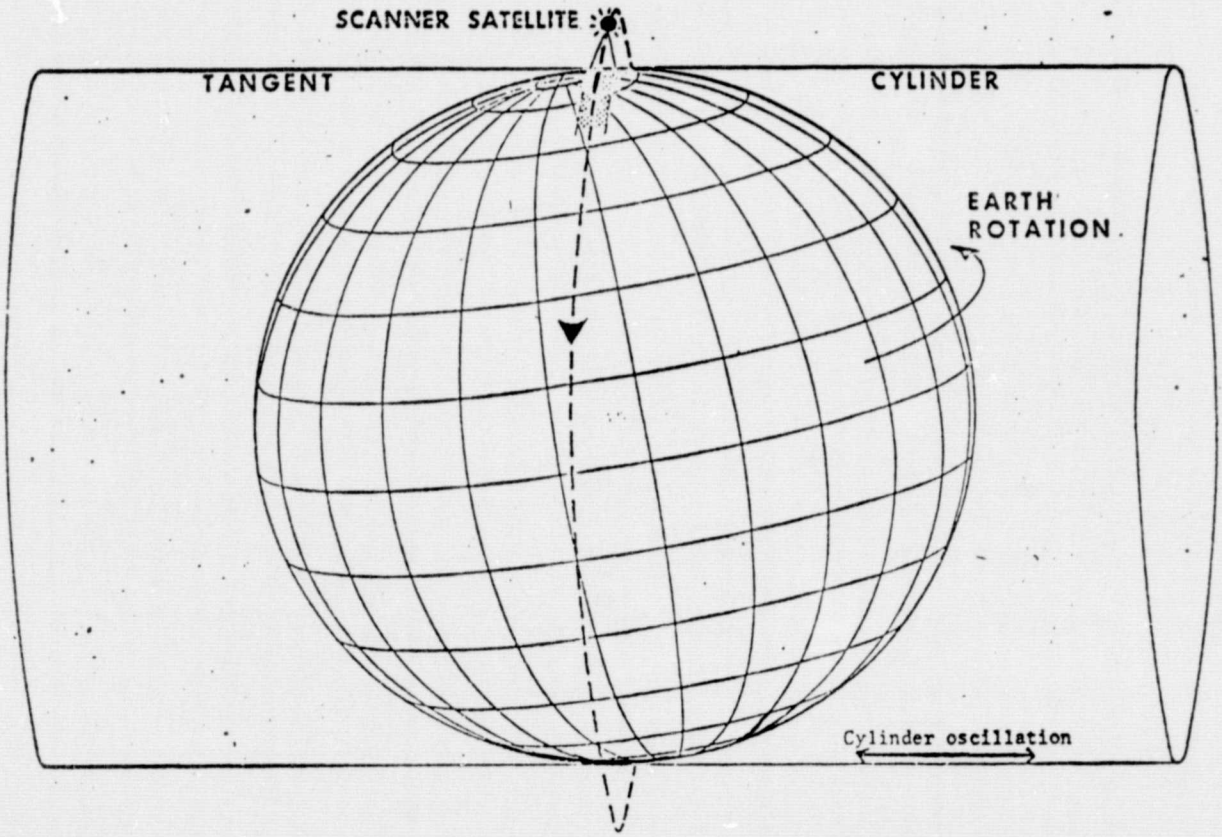

Figure 3-3. Space Oblique Mercator Projection

The Lambert Conformal Conic (LCC) is the projection of the Earth spheroid onto a cone whose axis coincides with the polar axis of the spheroid as shown in Figure 3-4. (from Reference 13). The cone is secant to the Earth, intersecting along two parallels of latitude which are on the same side of the equator. Meridians appear as straight lines radiating from a point beyond the mapped area. Latitude parallels appear as arcs of concentric circles which are centered at the point from which the meridians radiate.

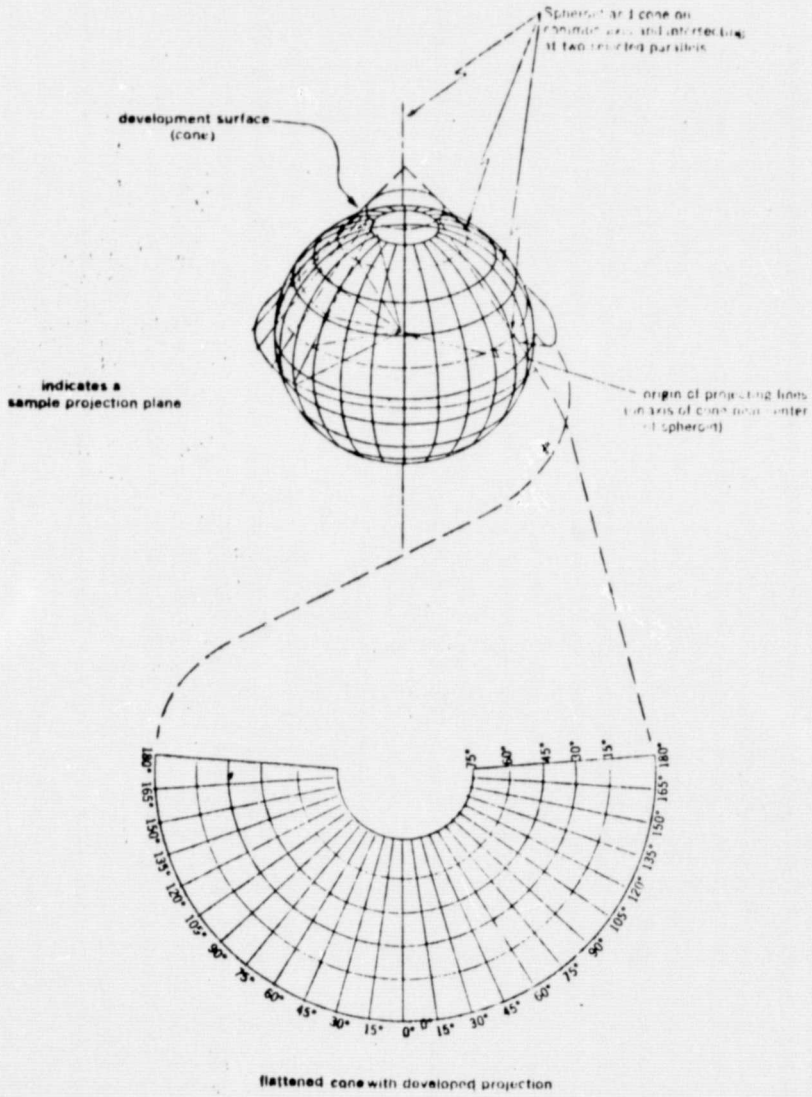

Figure 3-4. Lambert Conformal Conic Projection

One slight problem with UTM and LCC projections is that the scan lines of image data will not be normal to the north vector. This is illustrated in Figure 3-5 for the case at the equator. In order to project the scan lines normal to a north vector it is necessary to rotate them through ever increasing angles as latitude increases. The cost of a rotational buffer increases rapidly with latitude also, as shown in Figure 3-6. The savings in hardware cost outweigh the minor disadvantages of not rotating scan lines. Film products will simply be manually rotated to overlay on maps. Slight discontinuities in producing mosaics from high-latitude, non-parallel ground tracks will result. Digital map registration will require user applied rotations, but these should involve significantly less data and smaller buffer costs. Thus, the Landsat D system will rotate scan lines for yaw and alignment biases only, which have a much smaller cost impact since the angle is approximately ±0.10 degrees.

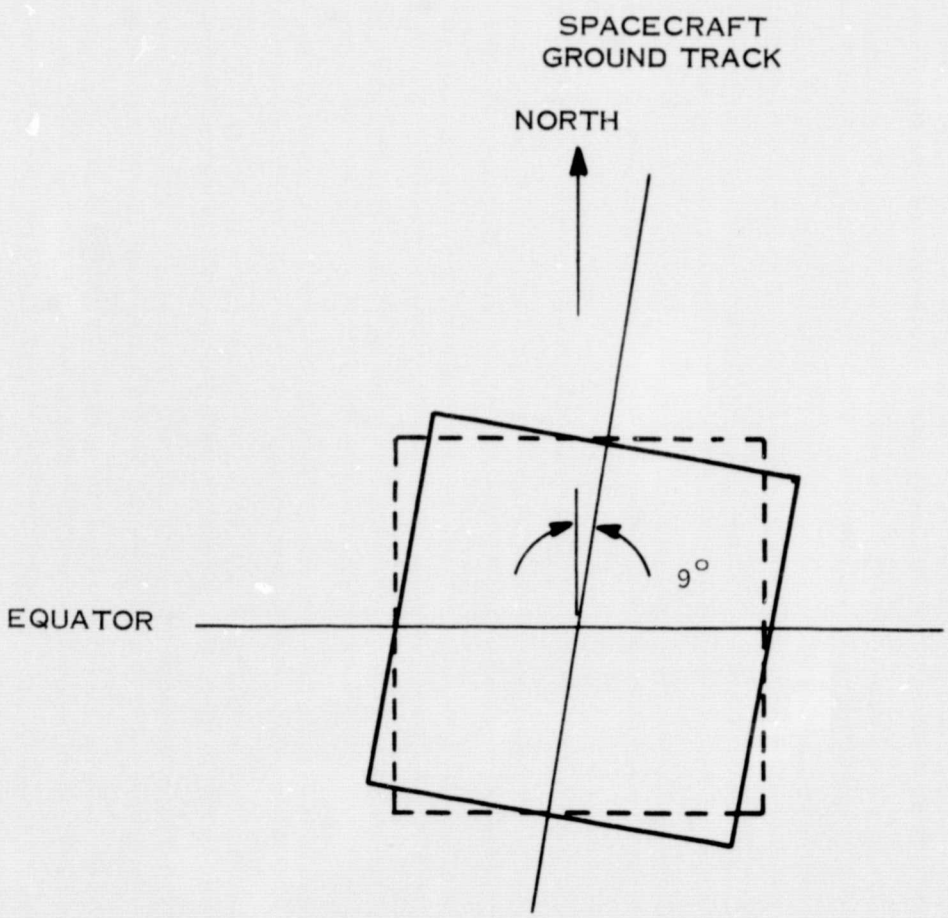

Figure 3-5. Scene Orientation at Equator

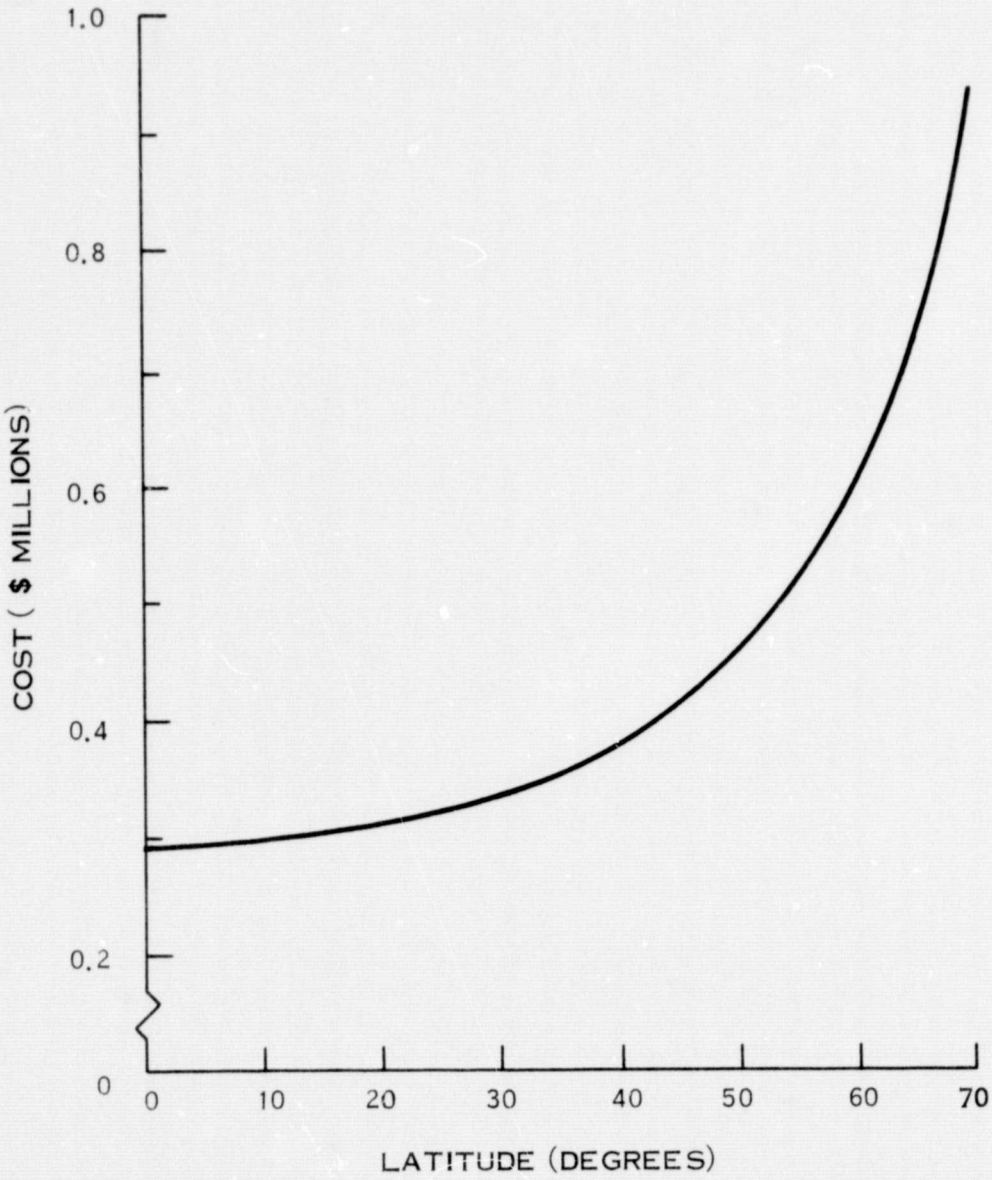

Figure 3-6. Rotational Buffer Cost

SECTION 4

CONCLUSIONS

Since the Landsat D System will utilize the Multi-mission Modular Spacecraft, ACS pointing and rate errors are significantly less than those produced by former Landsat spacecraft. The MMS stability permits control point processing and correction of the imagery on a per swath basis. Per swath correction minimizes processing complexity and the amount of hardware required.

Since ephemeris errors are small compared to ACS and alignment inaccuracies and best fit ephemeris is not significantly better than predicted, the predicted ephemeris will be used. This offers advantages because correction processing is not delayed by the best fit computations and can be available in near real time.

A choice of map projections may be offered to the users since no one projection will satisfy all users. This approach is the most flexible way to insure user satisfaction. UTM and LCC map projections could require scan line rotations in order to orient them normal to a north vector. However, the rapidly rising buffer costs incurred by large rotations is a strong deterrent. Significant cost savings coupled with a clear lack of universal user preference has driven the decision not to rotate scan lines for map projections.

REFERENCES

REFERENCES

1. Specification for Multi-mission Modular Spacecraft Attitude Control System, GSFC-S-700-17, April, 1976.

2. Landsat Prediction Error Growth, Mrs Ellen Herring, Operational Orbit Support Branch, OSCD, September 12, 1975.

3. Preliminary Error Analysis for the Landsat-C Satellite, T. Jones, Wolf Research and Development, March, 1976.

4. Telecon with Mrs. Ellen Herring, Operational Orbit Support Branch, GSFC, July 1, 1976.

5. ERTS Data Users Handbook, GE Doc. No. 71SD 249, 1 December 1972.

6. Earth Observatory Satellite System Definition Study Report No. 5, Vol. 2, EOS-A System Specification, GE Document No. 74SD4249, 16 September 1974.

7. All-Digital Precision Processing of ERTS Images, R. Bernstein, Final Report NAS5-21716, April 1975.

8. Digital Image Registration Study, TIS No. 72SD236, D. Nicholson and R. Economy, 21 March 1972. (internal GE Document)

9. Radiometric Resampling for Digital Image Correction, TIS No. 75SD5028, G. Liebling and W. Guard, 1 November 1975. (internal GE Document)

10. EOS Attitude Control/Ground System Study, IBM Federal Systems Division, NAS5-21947, 26 September 1973.

11. LANDSAT Digital Image Rectification System Preliminary Documentation, Van Wie, Stein, Puccinelli and Fields, GSC-12156, November 1975.

12. Space Oblique Mercator, Photogrammetric Engineering, A. Colvocoresses, August 1974.

13. Grids and Grid References, Technical Manual No. 5-241-1, Headquarters Department of the Army, 7 June 1967.